4-23-2022

PICKLE Associates With Histone Deacetylase 9 to Mediate Vegetative Phase Change in *Arabidopsis*

Tieqiang Hu

Darren Manuela

Valerie Hinsch

Mingli Xu
University of South Carolina, minglixu@sc.edu

Publication Info

Published in *New Phytologist*, Volume 235, Issue 3, 2022, pages 1070-1081.

Research

New Phytologist

PICKLE associates with histone deacetylase 9 to mediate vegetative phase change in *Arabidopsis*

Tieqiang Hu, Darren Manuela, Valerie Hinsch and Mingli Xu

Department of Biological Sciences, University of South Carolina, Columbia, SC 29208, USA

Author for correspondence:
Mingli Xu
Email: minglixu@sc.edu

Received: *24 January 2022*
Accepted: *9 April 2022*

New Phytologist (2022) **235:** 1070–1081
doi: 10.1111/nph.18174

Key words: *Arabidopsis*, H2Aub, H3K27ac, H3K27me3, HDA9, miR156, PKL, vegetative phase change.

Summary

- The juvenile-to-adult vegetative phase change in flowering plants is mediated by a decrease in miR156 levels. Downregulation of *MIR156A/MIR156C*, the two major sources of miR156, is accompanied by a decrease in acetylation of histone 3 lysine 27 (H3K27ac) and an increase in trimethylation of H3K27 (H3K27me3) at *MIR156A/MIR156C* in *Arabidopsis*.
- Here, we show that histone deacetylase 9 (HDA9) is recruited to *MIR156A/MIR156C* during the juvenile phase and associates with the CHD3 chromatin remodeler PICKLE (PKL) to erase H3K27ac at *MIR156A/MIR156C*.
- H2Aub and H3K27me3 become enriched at *MIR156A/MIR156C*, and the recruitment of Polycomb Repressive Complex 2 (PRC2) to *MIR156A/MIR156C* is partially dependent on the activities of PKL and HDA9.
- Our results suggest that PKL associates with histone deacetylases to erase H3K27ac and promote PRC1 and PRC2 activities to mediate vegetative phase change and maintain plants in the adult phase after the phase transition.

Introduction

During the vegetative development of flowering plants, the shoot produces morphologically distinct leaves (juvenile and adult leaves) before flowering (Poethig, 2003, 2013). The juvenile-to-adult phase transition (vegetative phase change) is largely controlled by the conserved miR156-SPL module (Willmann & Poethig, 2007; Wu *et al.*, 2009; Wang *et al.*, 2011; Leichty & Poethig, 2019), which also regulates floral induction, the immune response, herbivore resistance, and grain development (Jiao *et al.*, 2010; Mao *et al.*, 2017; Wang *et al.*, 2018; Hyun *et al.*, 2019). Transcription of *MIR156A/MIR156C*, the two major sources of mature miR156 in *Arabidopsis*, is controlled by epigenetic factors (Picó *et al.*, 2015; Xu *et al.*, 2016a; Y. Xu *et al.*, 2016; Xu *et al.*, 2018; Fouracre *et al.*, 2021), components of the Mediator complex such as CENTER CITY (CCT)/MEDIATOR12 (MED12) and GRAND CENTRAL (GCT)/MED13 (Gillmor *et al.*, 2014; Buendía-Monreal & Gillmor, 2017), carbohydrates (L. Yang *et al.*, 2013; Yu *et al.*, 2013; Lawrence *et al.*, 2020; Xu *et al.*, 2021) and hormones such as ABA and hormone-related factors (Guo *et al.*, 2017, 2021; Tian *et al.*, 2020).

Among the epigenetic factors involved in transcriptional regulation of *MIR156A/MIR156C* are the CHD3 chromatin remodeler, PICKLE (PKL) and the SWI2/SNF2 ATPase, BRAHMA (BRM). PICKLE promotes, while BRM prevents, the formation of nucleosomes near the transcription start site (TSS) of *MIR156A/MIR156C* (Xu *et al.*, 2016a; Y. Xu *et al.*, 2016). In addition to modulating chromatin structure, PKL also promotes trimethylation of lysine 27 on H3 (H3K27me3) at a variety of targets (Zhang *et al.*, 2008, 2012; Xu *et al.*, 2016a), while BRM has been reported to prevent H3K27me3 deposition at various targets (Li *et al.*, 2015; Y. Xu *et al.*, 2016). H3K27me3 is catalysed by Polycomb Repressive Complex 2 (PRC2), which is generally associated with transcriptionally repressed genes (Zhang *et al.*, 2007a; Lafos *et al.*, 2011; Li *et al.*, 2015). BRM occupancy prevents the association of PRC2, therefore preventing the deposition of H3K27me3 (Li *et al.*, 2015). It is however unknown how PKL promotes H3K27me3 deposition.

Most of the genes encoding PRC2 components are not expressed in a temporally changing pattern during vegetative development. However, the FERTILIZATION INDEPENDENT ENDOSPERM (FIE) protein, which is a component of all PRC2 complexes in *Arabidopsis*, is temporally associated with *MIR156A/MIR156C* chromatin, indicating that PRC2 is temporally recruited to these genes (Xu *et al.*, 2016a). H3K27me3 may be promoted by decreasing H3K4me3 levels, as H3K4me3 levels at *MIR156A/MIR156C* are inversely correlated with H3K27me3 levels. H3K4me3 is catalysed by the SET domain protein ARABIDOPSIS TRITHORAX RELATED 7 (ATXR7) and promoted by the SWR1 complex whose activity promotes the exchange of histone variant H2A.Z for H2A (Tamada *et al.*, 2009; Choi *et al.*, 2013; Xu *et al.*, 2018). Mutation in the SWR1 complex resulted in decreased levels of H3K4me3 at both *MIR156A* and *MIR156C*, and increased levels of H3K27me3 at *MIR156A* but not at *MIR156C*. This suggests that reducing H3K4me3 levels is not sufficient to promote H3K27me3. PRC1 and PRC2 are co-localised at transcriptionally repressed genes, and the B3 transcription factor VIVIPAROUS/ABI3-LIKE (VAL1) and VAL2 can recruit PRC1 to these loci (Turck *et al.*,

2007; Zhang *et al.*, 2007b; C. Yang *et al.*, 2013). During epigenetic silencing of *FLOWERING LOCUS C* (*FLC*), VAL1 triggers the deposition of H3K27me3 at *FLC* and consequently repression of *FLC* (Qüesta *et al.*, 2016). VAL1 and VAL2 and the PRC1 RING finger protein *Arabidopsis thaliana* B LYMPHOMA MO-MLV INSERTION REGION 1A/1B (AtBMI1A/1B) mediate ubiquitination of H2A (H2Aub) and H3K27me3 at *MIR156A/MIR156C* (Picó *et al.*, 2015; Fouracre *et al.*, 2021). However, VAL1/2 regulate the overall levels rather than the temporal pattern of *MIR156A/MIR156C* expression (Fouracre *et al.*, 2021), leaving the factors that regulate the temporal recruitment of PRC2 to *MIR156A/MIR156C* to be determined.

Whereas trimethylation of H3K27 represses transcription, acetylation of this residue has the opposite effect. Consistent with this general observation, the level of H3K27ac at *MIR156A/MIR156C* is high during the juvenile phase, and declines as the shoot ages (Xu *et al.*, 2016a). HISTONE DEACETYLASE 9 (HDA9) erases H3K27ac globally (Chen *et al.*, 2016; Kim *et al.*, 2016; Zeng *et al.*, 2020), and the removal of the acetyl group at H3K27 is a prerequisite for trimethylation of H3K27 at *FLC* (Zeng *et al.*, 2020). HDA9 physically interacts with the SANT (SWI3/DAD2/N-CoR/TFIII-B) domain protein POWERDRESS (PWR) to regulate flowering (Kim *et al.*, 2016) and to promote the onset of age-related and dark-induced leaf senescence (Chen *et al.*, 2016). HIGH EXPRESSION OF OSMOTICALLY RESPONSIVE GENES 15 (HOS15) is another component of the HDA9–PWR complex and has similar roles in plant development in addition to immune and stress responses (Mayer *et al.*, 2019; Park *et al.*, 2019; Yang *et al.*, 2020). HDA9 also promotes thermomorphogenesis by assisting in eviction of H2A.Z at the auxin biosynthesis gene *YUCCA8* (*YUC8*), and in the deacetylation of H3K9K14 at the *YUC8* locus (van der Woude *et al.*, 2019).

In plants, the CHD3/4 chromatin remodeler PKL has been reported to regulate root cell differentiation, flowering, seedling differentiation, and vegetative phase change through modulating levels of H3K27me3 at targets (Li *et al.*, 2005; Zhang *et al.*, 2008, 2012; Aichinger *et al.*, 2009, 2011; Xu *et al.*, 2016a). PICKLE also has roles in reducing H3K27ac levels at some targets (Zhang *et al.*, 2012; Xu *et al.*, 2016a). However, PKL was reported to primarily exist as a monomer (Ho *et al.*, 2013), and how PKL acts to reduce H3K27ac and increase H3K27me3 has not been determined. Here we show that HDA9 is temporally recruited to *MIR156A/MIR156C*, and it associates with PKL to decrease H3K27ac levels and increase H2Aub and H3K27me3 levels at *MIR156A/MIR156C* to mediate vegetative phase change. Our results suggest the presence of a PKL–HDA9 complex and further suggest that this complex promotes the activities of PRC1 and PRC2 at *MIR156A/MIR156C* chromatin.

Materials and Methods

Plant material and growth conditions

All the *Arabidopsis* stocks used in this study were on the Col background. *pkl-10*, *swn-3* have been described previously (Xu *et al.*, 2016a). *hda6-7* (cs66154) and *hda9-1* (SALK_007123) were obtained from the ABRC. Fragments of the FIE promoter and coding region were cloned using the Golden Gate method (Engler *et al.*, 2014) and a 6×HA tag was inserted after the FIE coding region (Wood *et al.*, 2006; Deng *et al.*, 2013). The *FIE-HA* construct was then transformed into *fie-11* heterozygotes, and plant homozygous for *fie-11* with a wild-type phenotype was selected for FIE binding assays. Similarly, *HDA6-HA*, *HDA6-GFP*, *HDA9-HA*, *HDA9-GFP* and *PKL-GFP* lines were constructed by the Golden Gate system and transformed into *hda6-7*, *hda9-1* or *pkl-10* mutants. Lines that have complemented the corresponding *hda6-7*, *hda9-1* and *pkl-10* mutant were selected for western blot, co-immunoprecipitation (Co-IP) and chromatin IP (ChIP) analysis. Seeds were sown on Sunshine SS#8F2 potting soil, stratified at 4°C for 2–4 d, and then transferred to Conviron growth chambers maintained at a constant 22°C in either LDs (16 h : 8 h, light : dark) or short-days (SD) (10 h : 14 h, light : dark). Unless otherwise specified, all of the data presented in this article were obtained from plants growing under SDs. Plant age was measured from the date when pots were transferred to growth chambers.

Quantitative RT-PCR

Shoot apices of SD grown plants were harvested and total RNA from them was extracted using TRIzol reagent (Invitrogen), followed by Turbo DNase (Ambion) treatment, according to the manufacturer's instructions. cDNA was reverse transcribed from 1 μg of RNA using SuperScript III reverse transcriptase (Invitrogen), and qPCR was performed using a Bio-Rad CFX96 real-time system. Primers used for qPCR are listed in Supporting Information Table S1.

Co-immunoprecipitation

HDA6-HA hda6-7 and *HDA9-HA hda9-1* were crossed to *PKL-GFP pkl-10* and plants homozygotes for each were selected for Co-IP analysis. In total, 1 g of seedlings from each genotype was ground in liquid nitrogen and 2 ml of extraction buffer (50 mM pH 7.5 Tris–HCl, 150 mM NaCl, 1 mM DTT, 1 mM EDTA, 5 mM $MgCl_2$, 1.5 mM $CaCl_2$, 1 mM PMSF, 0.5% NP-40 detergent, 10% glycerol, Protease Inhibitor Cocktail Sigma P9599) were added to the fine powder. The crude extract was centrifuged twice at 17 000 ***g*** for 10 min. The supernatant after centrifugation was then collected for IP assays. Next, 25 μl GFP-Trap magnetic beads (Chromotek, Islandia, NY, USA) were added to each tube for IP and gently rocked overnight at 4°C. The beads were then washed with washing buffer (50 mM pH 7.5 Tris–HCl, 150 mM NaCl, 1 mM EDTA, 0.5% NP-40 detergent, 10% glycerol) three times and eluted with 1× reduced Laemmli sample buffer. The eluted substances, as well as inputs, were subjected to western blot analysis. Antibodies against HA (12CA5; Sigma) and GFP (A11122; Invitrogen) were used as the primary antibodies in western blot analysis, followed by HRP-linked anti-rabbit IgG (7074; Cell Signalling, Danvers, MA, USA) or HRP-linked anti-mouse IgG (7076; Cell Signalling) as secondary antibodies. The membrane was incubated using Amersham Western

Blotting Detection Reagents and detected using the Amersham ImageQuant 800 system.

Chromatin immunoprecipitation

Here, 0.5–1.0 g 1-wk-old, 2-wk-old, or 3-wk-old shoot apices were harvested and fixed with 1% formaldehyde under vacuum for 15 min. Tissues were ground in liquid nitrogen and suspended in extraction buffer 1 (0.4 M sucrose, 10 mM Tris–HCl, pH 8.0, 10 mM $MgCl_2$, 5 mM β-mercaptoethanol, 1 mM PMSF, and 0.1% Triton X-100). Pellets were washed with extraction buffer 2 (0.25 M sucrose, 10 mM Tris–HCl, pH 8.0, 10 mM $MgCl_2$, 5 mM β-mercaptoethanol, 1 mM PMSF, and 1% Triton X-100), and resuspended in nuclei lysis buffer (50 mM Tris–HCl, pH 8.0, 10 mM EDTA and 1% SDS). DNA was then diluted in buffer (1.2 mM EDTA, 16.7 mM Tris–HCl, pH 8.0, 167 mM NaCl and 0.01% SDS) and sonicated using a Covaris ultrasonicator M220. Next, 1% of antibodies against HA (12CA5; Sigma), GFP (A11122; Invitrogen), H3 Abcam (ab1791, Waltham, MA, USA), H3K27me3 Millipore (07-449), H3K27ac Abcam (ab4729) or H2Aub (8240S; Cell Signalling) were used in IP. The IP protein and DNA were reverse crosslinked, and DNA was isolated using the QIA Quick PCR purification kit (Qiagen). qPCR was performed on a Bio-Rad CFX96 real-time system after DNA was extracted from the IP product. For H3K27me3 and H3K27ac, STM was used as a control locus (Angel *et al.*, 2011; Coustham *et al.*, 2012; Qüesta *et al.*, 2016; Xu *et al.*, 2016a; Fouracre *et al.*, 2021), and data are presented as a ratio of (H3K27me3 gene of interest/H3 gene of interest) to (H3K27me3 STM/H3 STM) or (H3K27ac gene of interest/H3 gene of interest) to (H3K27ac STM/H3 STM). For H2Aub, ABI3 was used as a control locus (C. Yang *et al.*, 2013; Qüesta *et al.*, 2016; Fouracre *et al.*, 2021) and data are presented as the ratio of (H2Aub gene of interest/H3 gene of interest) to (H2Aub ABI3/H3 ABI3). For GFP ChIP, TA2 was used as a control locus and data are presented as the ratio of (GFP ChIP gene of interest/GFP input gene of interest) to (wild-type ChIP gene of interest/wild-type input gene of interest) normalised to the TA2 locus. Fold enrichment in the HDA6-HA ChIP analysis was calculated following the same procedure as in the GFP ChIP analysis. Primers for ChIP analysis are listed in Table S1.

Western blot

Nuclear proteins were isolated from 2-wk-old Col, *pkl-10*, *hda9-1* and *pkl-10 hda9-1* using the same extraction buffer 1, extraction buffer 2 and nuclei lysis buffer as used for ChIP analysis. The nuclear proteins were resolved on a 4–12% SDS-PAGE gradient gel and transferred to a membrane. The membrane was incubated with anti-H3 (ab1791), anti-H3K27ac (ab4729), anti-H3K27me3 (07-449; Millipore), and H2Aub (8240S; Cell Signalling) as first antibodies, followed by HRP-linked anti-rabbit IgG (7074; Cell Signalling) as the secondary antibody. The membrane was incubated using Amersham Western Blotting Detection Reagents and detected and analysed on the Amersham ImageQuant 800 system.

Results

HDA6 and HDA9 promote vegetative phase change through miR156-independent and miR156-dependent pathways, respectively

The juvenile-to-adult vegetative phase transition is mediated by the downregulation of pri-miR156a and pri-miR156c, the two major sources of mature miR156 (Wu *et al.*, 2009; Xu *et al.*, 2016a,b; He *et al.*, 2018). The downregulation of pri-miR156a and pri-miR156c is correlated with a decrease in H3K27ac and an increase in H3K27me3 at *MIR156A/MIR156C* (Xu *et al.*, 2016a). Previous work has shown that the CHD3 chromatin remodeler PKL promotes a decrease in H3K27ac and an increase in H3K27me3 at these loci (Xu *et al.*, 2016a), but its mechanism remains unknown. HDA6 and HDA9 are reported to remove histone acetylation and to induce downregulation of gene expression in plants (Probst *et al.*, 2004; Earley *et al.*, 2006; Tanaka *et al.*, 2008; van Zanten *et al.*, 2014; Chen *et al.*, 2016; Kim *et al.*, 2016; Mayer *et al.*, 2019; Zeng *et al.*, 2020). To determine if these genes play a role in vegetative phase change, we examined the phenotype of the null alleles *hda6-7* (*rts1-1*) (Aufsatz *et al.*, 2002) and *hda9-1* (van Zanten *et al.*, 2014; Chen *et al.*, 2016; Kim *et al.*, 2016). In *Arabidopsis*, juvenile shoots have a relatively short plastochron and produce leaves that are relatively small and round and lack trichomes on their abaxial surface, whereas adult shoots have a longer plastochron and produce leaves that are larger, more elongated and have trichomes on their abaxial surface (Telfer *et al.*, 1997; Wang *et al.*, 2008; Wu *et al.*, 2009). The rosette of *hda6-7* resembled wild-type Col, whereas the rosette of *hda9-1* was slightly smaller and had more leaves than Col rosettes of the same age, demonstrating that *hda9-1* has a shorter plastochron than Col (Fig. 1a). Under SD conditions, the first leaf with abaxial trichomes in Col was leaf 8.4, and was delayed by *c.* 2 leaves in *hda6-7* and 4 leaves in *hda9-1* (Fig. 1b). Abaxial trichome production in *hda6-7 hda9-1* was not significantly different from *hda9-1* (Fig. 1b). Juvenile leaves are rounder and have a smaller leaf blade length : width ratio than the adult leaves (Xu *et al.*, 2016a,b; He *et al.*, 2018). The leaf blade length : width ratio of the 5th and 7th leaves of *hda9-1* was significantly smaller than that of the 5th and 7th leaves of Col, while the leaf blade length : width ratio of the 5th and 7th leaves of *hda6-7* was not significantly different from Col; there was no significant difference in the length : width ratio of *hda9-1* and *hda6-7 hda9-1* (Fig. 1a,c). These results suggested that HDA6 and HDA9 regulated vegetative phase change by different mechanisms.

To investigate if HDA6 and HDA9 regulated vegetative phase change by modulating the amount of miR156, we used RT-qPCR to examine the level of miR156 in the shoot apices of Col, *hda6-7*, *hda9-1*, and *hda6-7 hda9-1* at 8, 12, 16 and 20 d after planting. *hda6-7* had no effect on the level of miR156, but *hda9-1* and *hda6-7 hda9-1* had elevated levels of miR156 at each of these time points; the amount of miR156 in *hda6-7 hda9-1* was not significantly different from *hda9-1* (Fig. 1d). To determine if HDA6 and HDA9 affected the level of miR156 by controlling the transcription of *MIR156A/MIR156C*, we examined the

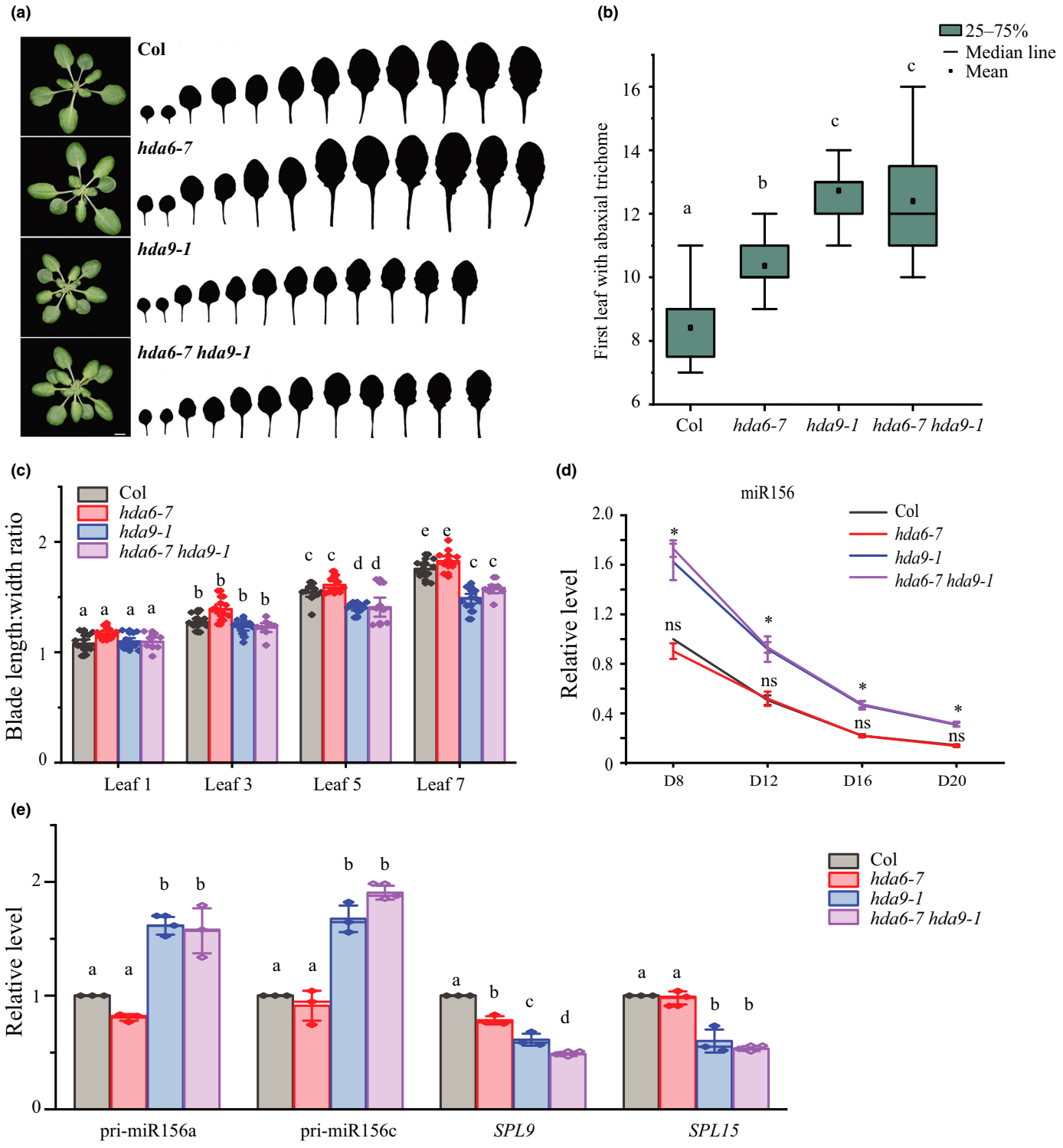

Fig. 1 HDA6 and HDA9 act in miR156-dependent and miR156-independent pathways to promote vegetative phase change in *Arabidopsis*. (a) Rosettes and successive leaves of Col, *hda6-7*, *hdad9-1*, and *hda6-7 hda9-1* grown under short-day (SD) conditions. Bar, 3 mm. (b) *hda6-7* and *hdad9-1* delay the production of abaxial trichomes in SDs. (c) The leaf blade length : width ratio in leaf 1, leaf 3, leaf 5 and leaf 7 of Col and mutants. (d) RT-qPCR analysis of temporal variation of miR156 in the shoot apices of Col and mutants. Values are relative to Col at day 8 and represent the mean ± SE from three biological replicates. *, Significant difference between *hda9-1* and Col, *hda6-7 hda9-1* and hda6-7, $P < 0.05$, one-way analysis of variance (ANOVA). ns, no significant difference between *hda6-7* and Col, $P > 0.05$, one-way ANOVA. (e) RT-qPCR analysis of pri-miR156a, pri-miR156c, *SPL9* and *SPL15* in Day 20 shoot apices of Col and mutants. Shared letters indicate not significantly different groups, different letters indicate significantly different groups, $P < 0.05$, one-way ANOVA. Comparison in (e) was performed within groups.

primary transcripts of these loci (pri-miR156a and pri-miR156c). Consistent with the results for miR156, pri-miR156a and pri-miR156c were significantly elevated in *hda9-1*, but were not significantly different from wild-type in *hda6-7* (Fig. 1e). Among the 10 miR156-targeted SPLs in *Arabidopsis*, SPL9 and SPL15 are important for vegetative phase change. These genes are repressed by miR156 through both transcript cleavage and translational repression (Xu *et al.*, 2016a,b; He *et al.*, 2018). *SPL9* transcripts were significantly reduced in both *hda6-7* and *hda9-1*, and were reduced more in *hda6-7 hda9-1* than in the single mutants (Fig. 1e). However, transcripts of *SPL15* were downregulated in *hda9-1* but not in *hda6-7*, and were downregulated to similar levels in the *hda9-1* single mutant and the *hda6-7 hda9-1* double mutant (Fig. 1e). These results suggested that HDA6 and HAD9 both regulated vegetative phase change, but through different mechanisms. HDA9 repressed the transcription of *MIR156A/MIR156C*, while HDA6 directly or indirectly promoted the transcription of *SPL9* independently of miR156, and may also regulate the downstream targets of SPL proteins.

HDA9 binds to *MIR156A* and *MIR156C* in a temporally regulated manner

To determine how HDA6 and HDA9 regulate vegetative phase change, we examined the expression patterns of the *HDA6* and *HDA9* transcripts, and whether these proteins were recruited to miR156 and *SPL* genes. The abundance of *HDA6* and *HDA9* transcripts was not significantly different in 1-wk-old to 3-wk-old Col shoot apices (Fig. S1a), indicating that the regulation of vegetative phase change by them is not due to the transcriptional regulation of *HDA6* and *HDA9*. To investigate the chromatin-binding patterns of these proteins, genomic constructs of *HDA6::HDA6* fused to *HA* (*HDA6::HDA6-HA*) and *HDA9::HDA9-GFP* were transformed into *hda6-7* and *hda9-1*, respectively, and transgenic lines in which these mutations were complemented were selected for further analysis (Fig. S2a,c,e,g). We used ChIP followed by qPCR (ChIP-qPCR) to examine if HDA6 bound to *SPL9*, as suggested by our observation that transcripts of *SPL9* are decreased in *hda6-7*. We observed no binding of HDA6 to the *SPL9* promoter or the region between the TSS and the second exon in 1-wk-old, 2-wk-old and 3-wk-old shoot apices (Fig. S1b,c).

We next examined the binding of HDA9 to *MIR156A/MIR156C* in 1-wk-old, 2-wk-old and 3-wk-old shoot apices. We found that HDA9-GFP bound to the promoter and transcribed regions of *MIR156A/MIR156C* (Fig. 2a–d) and was more strongly associated with the region after the TSS than the region before the TSS. This was consistent with the observation that H3K27ac was more abundant in the region after the TSS than in the promoter region of these genes (Xu *et al.*, 2016a). The association of HDA9 with *MIR156A/MIR156C* increased from 1 to 2 wk after planting, and declined from 2 to 3 wk. This was correlated with the greater decrease in H3K27ac from 1 to 2 wk after planting than from 2 to 3 wk (Fig. 2b,d) (Xu *et al.*, 2016a). Together, our results indicated that HDA6 regulates *SPL9* indirectly, independently of miR156, whereas HDA9 directly regulates *MIR156A/MIR156C*.

HDA9 associates with PKL to repress the transcription of *MIR156A/MIR156C*

PICKLE has activities in reducing H3K27ac levels at *MIR156A/MIR156C* chromatin, although PKL itself is a chromatin remodeler (Xu *et al.*, 2016a). To determine if PKL reduced H3K27ac levels through interacting with histone deacetylases, we investigated genetic interactions between these factors by crossing *pkl-10* to *hda6-7* and *hda9-1*. In SDs, the first leaf with the abaxial trichome in Col was leaf 7.5, whereas it was leaves 10, 11.1 and leaf 12.2 in *hda6-7*, *hda9-1* and *pkl-10*, respectively. In the *pkl-10 hda6-7* and *pkl-10 hda9-1* double mutants, the first leaf with

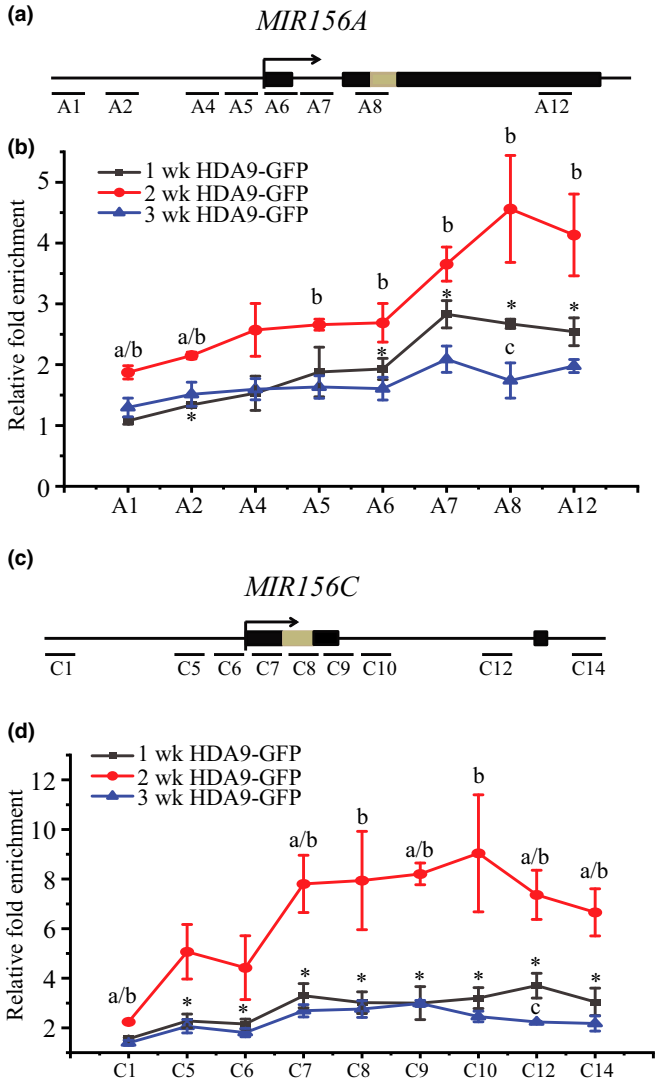

Fig. 2 HDA9 binds to *MIR156A* and *MIR156C* in a temporal manner. (a, c) Locations of the *MIR156A* (a) and *MIR156C* (c) genomic sites analysed by chromatin immunoprecipitation-quantitative polymerase chain reaction (ChIP-qPCR). The miR156 hairpin is coloured light brown. (b, d) Anti-GFP ChIP analysis of HDA9-GFP binding to *MIR156A* (b) and *MIR156C* (d) in 1, 2 and 3 wk tissue. Values represent the mean ± SE from three biological replicates. a, significant difference between 1 and 2 wk; b, significant difference between 2 and 3 wk; c, significant difference between 1 and 3 wk. *, Significant difference between the transgenic plant and Col at 1 wk. $P < 0.05$, *t*-test.

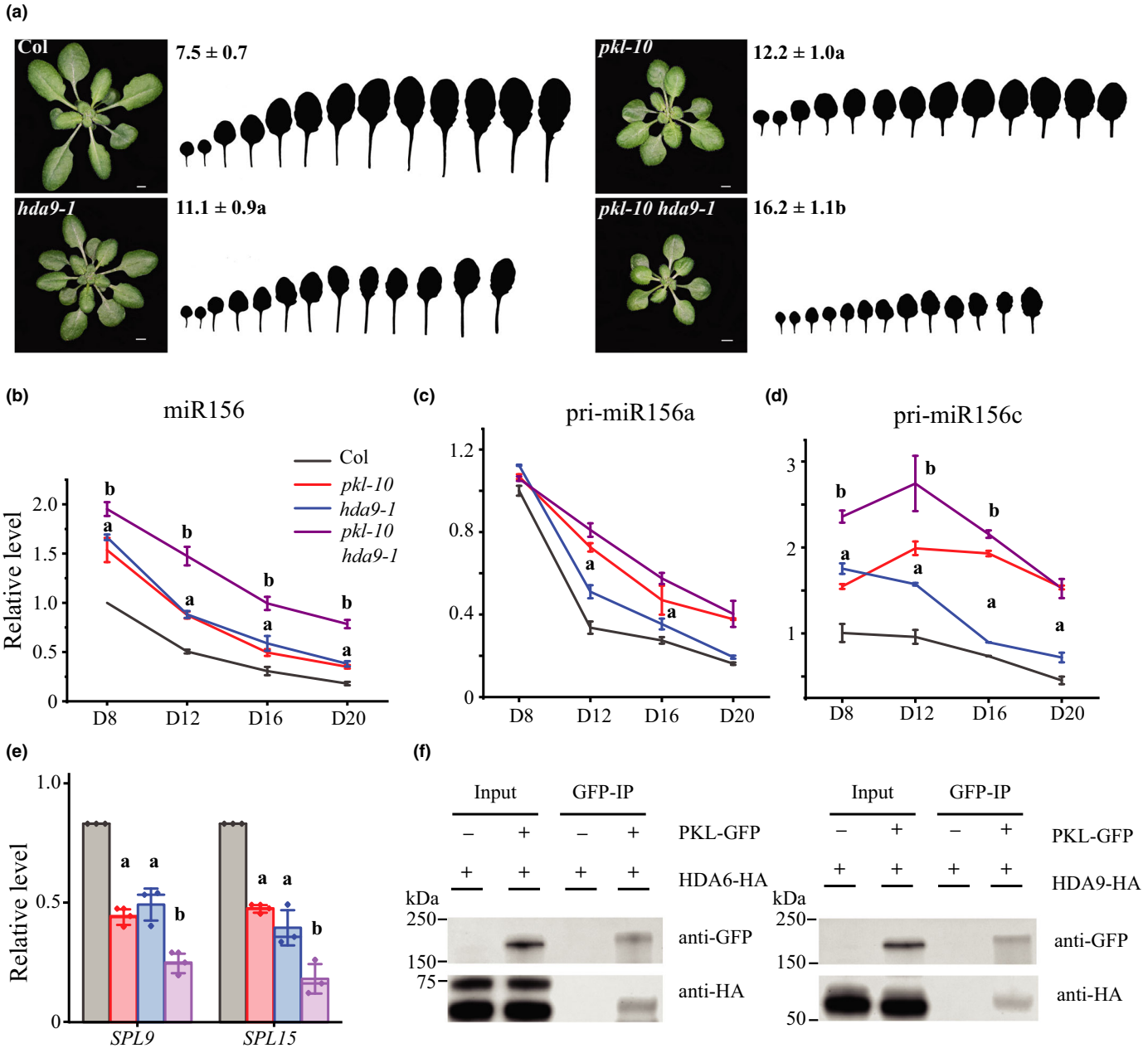

Fig. 3 PKL and HDA9 associate to promote vegetative phase change. (a) Rosettes and successive leaves of Col, *pkl-10*, *hdad9-1* and *pkl-10 hda9-1* grown under short day (SD) conditions. Bar, 3 mm. Numbers represent the first leaf with abaxial trichome in Col and mutants (data are means ± standard deviation from 32 plants for each genotype). (b–d) RT-qPCR analysis of temporal variation of miR156 (b), pri-miR156a (c), and pri-miR156c (d) levels in the shoot apices of Col and mutants. Values are relative to Col at day 8 and represent the mean ± SE from one biological replicate. (e) RT-qPCR analysis of *SPL9* and *SPL15* transcripts in 20-d-old shoot apices of Col and mutants. Values are relative to Day 20 Col and represent the mean ± SE from three biological replicates. a, significant difference between Col and the single mutants; b, significant differences between the single mutants and the double mutant. $P < 0.05$, one-way ANOVA. (f) Co-immunoprecipitation (Co-IP) analysis of PKL-GFP and HDA6-HA as well as PKL-GFP and HDA9-HA in *Arabidopsis*.

abaxial trichomes was leaf 21.5 and leaf 16.2, respectively (Figs 3a, S3a), indicating that PKL interacted synergistically with HDA6 and additively with HDA9. We then examined the levels of miR156 in these single mutants and double mutants. RT-qPCR showed that in 8-d-old plants miR156 was elevated *c.* 50% in the *pkl-10* and *hda9-1* single mutants and by *c.* 100% in the *pkl-10 hda9-1* double mutant (Fig. 3b) and was reduced in both the single and double mutants as plants aged (Fig. 3b). By contrast, the level of miR156 in the *pkl-10 hda6-7* double mutant was similar to the level in *pkl-10* (l Fig. S3b). This was consistent with our observation that *hda6-7* did not affect the level of miR156 (Fig. 1d). RT-qPCR analysis of the pri-miR156a transcript showed that Col, *pkl-10*, *hda9-1* and *pkl-10 hda9-1* had similar amounts of this transcript at 8 d after planting, but that it subsequently decreased more slowly in *hda9-1*, *pkl-10* than in Col (Figs 3c, S3c,e). pri-miR156c was more abundant in *pkl-10*,

hda9-1 and *pkl-10 hda9-1* than in Col at day 8, then declined in *pkl-10 hda9-1* more slowly than in Col, *pkl-10*, or *hda9-1* (Figs. 3d, S3d,f). To determine if this difference in miR156 levels was functionally significant, we measured the abundance of the transcripts of two its targets, *SPL9* and *SPL15*. These transcripts were reduced to 40–50% of the wild-type level in *hda9-1* and *pkl-10*, and to 20–30% of the wild-type level in *pkl-10 hda9-1* (Fig. 3e). These results demonstrated that PKL and HDA9 contributed to the downregulation of pri-miR156a and pri-miR156c.

To determine if PKL decreased H3K27ac levels at *MIR156A/MIR156C* by physically interacting with histone deacetylases, we tested the association of PKL with HDA6 and HDA9 using a Co-IP assay. Constructs of *PKL::PKL*-GFP, *HDA6::HDA6-HA*, and *HDA9::HDA9-HA* were transformed into *pkl-10*, *hda6-7* and *hda9-1*, respectively, and transgenic lines in which the corresponding mutations were complemented were selected for further analysis (Fig. S2). *PKL::PKL-GFP pkl-10* was crossed to *HDA6::HDA6-HA hda6-7* and *HDA9::HDA9-HA hda9-1*, and plants homozygous for both transgenes and mutations were identified in F2 families derived from these crosses. Cell lysates of these lines were immunoprecipitated using an anti-GFP antibody, and GFP-associated proteins were subsequently subjected to western blot analysis using an anti-GFP antibody and an anti-HA antibody. HA-conjugated HDA6 or HDA9 were detected in the *PKL::PKL-GFP HDA6::HDA6-HA pkl-10 hda6-7* and *PKL::PKL-GFP HDA9::HDA9-HA pkl-10 hda9-1* samples, but not in the *HDA6::HDA6-HA hda6-7* or the *HDA9::HDA9-HA hda9-1* samples (Fig. 3f). This result suggested that PKL physically associates with HDA6 and HDA9 *in planta*.

HDA9 and PKL decrease H3K27ac and increase H3K27me3 and H2Aub at *MIR156A/MIR156C*

To determine how the PKL–HDA9 complex is involved in the transcriptional regulation of *MIR156A/MIR156C*, we examined the level of H3K27ac, H3K27me3 and H2Aub at these genes in the shoot apices of 1-wk, 2-wk and 3-wk-old wild-type plants and *pkl-10*, *hda9-1* and *pkl-10 hda9-1* mutants. Consistent with previous results (Xu *et al.*, 2016a), the level of H3K27ac was highest at 1 wk and declined as plants aged. The 1-wk-old *hda9-1* had higher levels of H3K27ac than Col at *MIR156_A6* and *MIR156_A7*, and the *pkl-10 hda9-1* double mutant had the highest level of H3K27ac at *MIR156_A6*, *MIR156_A7* and *MIR156_A10* (Fig. 4a–c). H3K27ac levels were significantly increased at *MIR156_C7* and *MIR156_C12* in 1-wk-old *pkl-10* and *hda9-1* single mutants, and the *pkl-10 hda9-1* double mutant had the highest levels of H3K27ac at *MIR156_C7*, *MIR156_C8* and *MIR156_C12* (Fig. 4d). This suggested that both PKL and HDA9 contribute to erasing H3K27 acetylation at *MIR156A/MIR156C*, and they had a bigger effect on *MIR156C* than *MIR156A*.

Next, we asked if the elevated level of H3K27ac at *MIR156A/MIR156C* in *pkl-10* and *hda9-1* was correlated with a decreased level of H3K27me3 at these genes. We found that the level of H3K27me3 at *MIR156_A6* was lower in 2-wk-old and 3-wk-old *pkl-10* mutants than in wild-type plants, but that there was no significant difference in H3K27me3 at *MIR156_A7* or at *MIR156_A10* (Fig. 4e). The levels of H3K27me3 at *MIR156_C7*, *MIR156_C8*, and *MIR156_C12* were lower than in the wild-type in 2-wk-old and 3-wk-old *pkl-10* plants (Fig. 4f). The *pkl-10 hda9-1* double mutant had a lower level of H3K27me3 than *pkl-10* at *MIR156_C7*, *MIR156_C8* and *MIR156_C12* (Fig. 4e,f). These results suggested that PKL and HDA9 functioned similarly in modulating H3K27ac, but had different functions in regulating H3K27me3 at *MIR156A/MIR156C*. HDA9 seems to have no role in regulating H3K27me3 at *MIR156A*, but acts with PKL to regulate H3K27me3 at *MIR156C*. This may explain why *pkl-10 hda9-1* had a larger effect on the expression of *MIR156C* than *MIR156A* (Fig. 3c,d).

Chromatin of *MIR156A/MIR156C* was also marked by H2A ubiquitination (H2Aub), which is catalysed by the activities of PRC1 (Picó *et al.*, 2015; Fouracre *et al.*, 2021). To determine if PKL and HDA9 affected the activities of PRC1, we examined the levels of H2Aub in Col, *pkl-10*, *hdda9-1* and *pkl-10 hda9-1* mutants. An analysis of H2Aub levels in wild-type plants showed that H2Aub decreased from 1 to 2 wk at *MIR156A*, but increased from 1 to 3 wk at *MIR156C* (Fig. 4g,h). H2Aub levels were significantly lower in 2-wk-old *pkl-10* or *hda9-1* single mutants than in the wild-type at both *MIR156A* and *MIR156C*, and H2Aub levels were lowest in *pkl-10 hda9-1* in 1-wk and 2-wk-old plants (Fig. 4g,h). These results indicated that PKL and HDA9 regulated H2Aub levels differently from the VAL1 transcription factor, which is uniformly present at *MIR156A/MIR156C* and regulated the overall amount of miR156 rather than the temporal decrease in miR156 during vegetative phase change (Fouracre *et al.*, 2021). Our results suggested that PKL and HDA9 modulation of H2A ubiquitination via PRC1 may precede the binding of PRC2, or be independent of PRC2, because mutations in these genes reduced H2Aub levels in 1-wk-old plants, but did not affect the level of H3K27me3 at this stage (Fig. 4e–h).

To investigate if PKL and HDA9 affected the levels of H3K27ac, H3K27me3 and H2Aub globally, we examined the overall levels of these marks in wild-type, *pkl-10*, *hda9-1* and *pkl-10 hda9-1* in three biological replicates. Nuclear proteins were isolated from 2-wk-old plants and assayed on western blots using anti-H3K27ac, anti-H3K27me3, anti-H2Aub and anti-H3 antibodies. Consistent with other reports, H3K27ac was elevated significantly in *hda9-1* and *pkl-10 hda9-1* (Kim *et al.*, 2016; Mayer *et al.*, 2019; Zeng *et al.*, 2020) but was not significantly affected by *pkl-10* (Figs 4i, S3). The global levels of H3K27me3 were not significantly reduced in *pkl-10* and *hda9-1* (Figs 4i, S3). However, the global levels of H2Aub were significantly reduced in *pkl-10*, *hda9-1* and *pkl-10 hda9-1* (Figs 4i, S4). Together, our results indicated that the histone deacetylase HDA9 erases acetylation on H3K27 globally. The chromatin remodeler PKL modulates the level of H3K27ac at specific genes, rather than globally and both PKL and HDA9 play a role in modulating H2Aub levels across the genome.

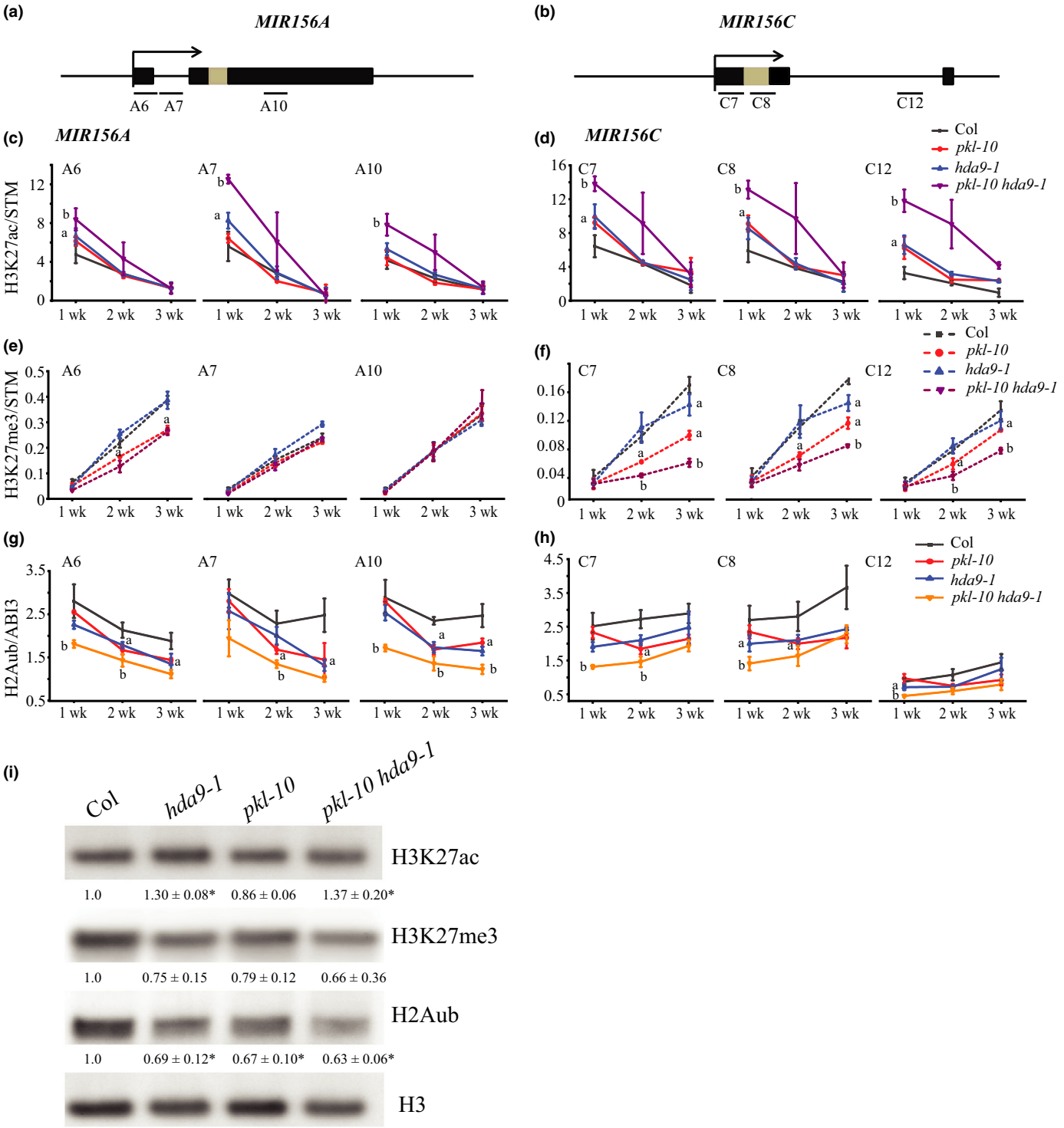

Fig. 4 PKL and HDA9 act together to promote deacetylation and methylation of H3K27, and ubiquitination of H2A at *MIR156A*/*MIR156C*. (a, b) Genomic locations of the *MIR156A* (a) and *MIR156C* (b) sites analysed by chromatin immunoprecipitation-quantitative polymerase chain reaction (ChIP-qPCR). The miR156 hairpin is coloured light brown. (c, d), ChIP-qPCR analysis of H3K27ac levels in 1-wk-old, 2-wk-old and 3-wk-old shoot apices of Col, *pkl-10*, *hda9-1*and *pkl-10 hda9-1*. (e, f), ChIP-qPCR analysis of H3K27me3 levels in the same tissue as in (c, d). (g, h), ChIP-qPCR analysis of H2Aub levels in the same tissue as in (c, d). Values (c–h) represent the mean ± SE from three biological replicates. a, significant difference between Col and the single mutants; b, significant differences between the single mutants and the double mutant. $P < 0.05$, one tailed, paired *t*-test. (i) Western blot analysis of H3K27ac, H3K27me3 and H2Aub in 2-wk-old shoot apices of Col, *pkl-10*, *hda9-1* and *pkl-10 hda9-1*. Folds compared with Col are normalised based on H3 levels. *, Significantly different from Col, $P < 0.05$, *t*-test. Values represent the mean ± SE from three biological replicates.

HDA9 acts to facilitate the binding of PRC2 at *MIR156A/MIR156C*

To investigate if PKL and HDA9 promoted the binding of PRC2 at *MIR156A/MIR156C*, we examined the binding of FIE to these genes in *pkl-10* and *hda9-1*. FIE is a homologue of the *Drosophila* PRC2 component, Esc, and is encoded by a single gene in *Arabidopsis* (Deng *et al.*, 2013). Previously, we found that FIE-HA (encoded by a *FIE::FIE-HA* transgene) was barely associated with *MIR156A/MIR156C* in 1-wk-old plants, but was present at these genes in 2-wk-old plants (Xu *et al.*, 2016a). We therefore examined the level of FIE-HA in wild-type, *pkl-10* and *hda9-1* in 2-wk-old plants. ChIP-qPCR analysis showed that *pkl-10* and *hda9-1* significantly affected the binding of FIE-HA at *MIR156_A6*, but did not affect the binding of FIE-HA at the other *MIR156A* sites we examined (Fig. 5a,b). PKL and HDA9 promoted the efficient association of FIE-HA with *MIR156C* more broadly, including at *MIR156_C5*, which is located before the TSS, and at *MIR156_C7*, *MIR156_C8*, *MIR156_C9*, which are located after the TSS. These results are consistent with the RT-qPCR analysis that there was more upregulation of pri-miR156c than pri-miR156a in *pkl-10* and *hda9-1* mutants (Fig. 3c,d).

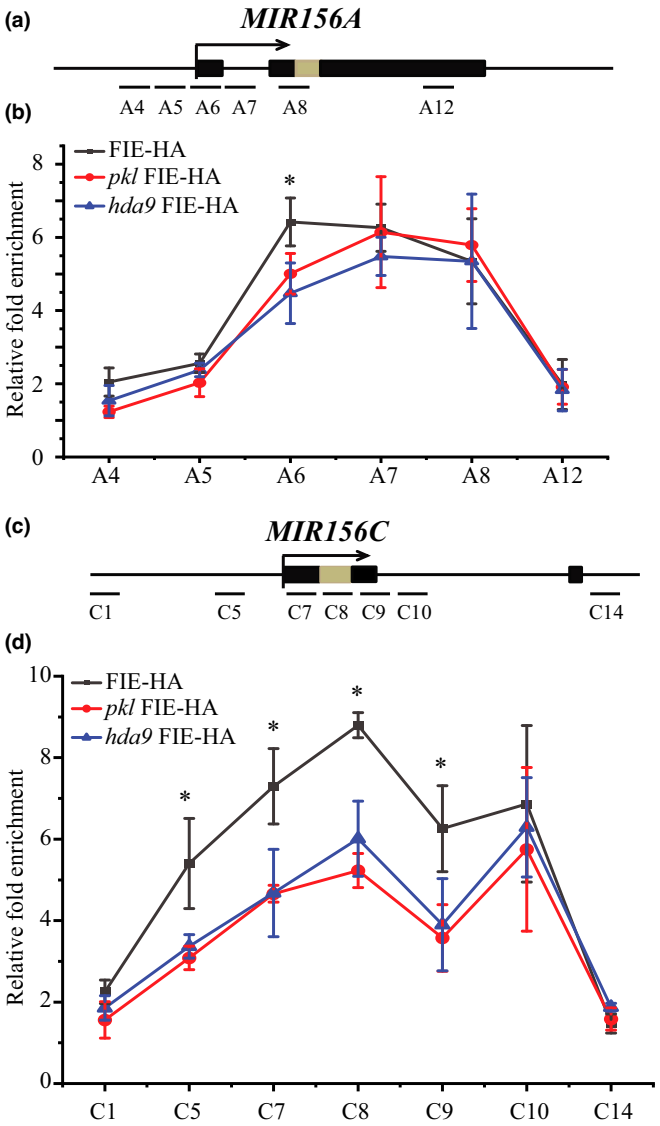

Fig. 5 PICKLE and HDA9 facilitate the binding of FIE to *MIR156A* and *MIR156C*. (a, c) Genomic locations of the *MIR156A* (a) *and MIR156C* (c) sites analysed by ChIP-qPCR. The miR156 hairpin is coloured light brown. (b, d) Anti-HA ChIP analysis of FIE-HA binding to *MIR156A* (b) and *MIR156C* (d) in 2-wk-old Col, *pkl-10* and *hda9-1*. Values represent the mean ± SE from three biological replicates. *, $P < 0.05$, one-way ANOVA.

Discussion

PKL associates with histone deacetylases

The juvenile-to-adult vegetative phase transition is an important decision in a plant's life cycle, as this developmental transition is associated with floral induction, immune response, herbivore resistance and grain development (Jiao *et al.*, 2010; Mao *et al.*, 2017; Wang *et al.*, 2018; Hyun *et al.*, 2019). miR156 is a master regulator for the juvenile phase and downregulation of miR156 promotes the juvenile-to-adult phase transition (Wu *et al.*, 2009; Xu *et al.*, 2016a). Understanding the mechanisms of how miR156 is transcriptionally downregulated and how this repression is maintained is important for understanding how vegetative phase change is promoted and maintained.

Our previous analysis showed that PKL modulates the *MIR156A/MIR156C* chromatin structure dynamically and PKL promotes the deacetylation and methylation of H3K27 at *MIR156A/MIR156C* during vegetative phase change (Xu *et al.*, 2016a). Here, we show that PKL physically associates with two histone deacetylases, HDA6 and HDA9, to mediate the juvenile-to-adult transition in *Arabidopsis*. Our analysis of the H3K27ac levels at *MIR156A/MIR156C* showed that 1-wk-old *hda9-1* had higher levels of H3K27ac than Col at both *MIR156A* and *MIR156C*, but that 1-wk-old *pkl-10* had higher levels of H3K27ac than Col at *MIR156C*, not *MIR156A*, suggesting that PKL and HDA9 function overlappingly and distinctively. Nevertheless, the H3K27ac levels were highest in the *pkl-10 hda9-1* double mutant at both *MIR156A* and *MIR156C*, suggesting that PKL function through HDA9 and other factors. PKL is a chromatin remodeler that modulates local chromatin structure to facilitate the recruitment of other factors (such as histone modifiers), and loss of PKL activity may result in the partial loss of the other factors' activities. Our co-IP analysis showed that PKL associates with HDA6 and HDA9, and that it could associate with other histone deacetylases to regulate H3K27ac levels and vegetative phase change in *Arabidopsis*.

HDA9 physically associates with plant SANT domain protein PWR and WD-40 protein HOS15 (Chen *et al.*, 2016; Kim *et al.*, 2016; Mayer *et al.*, 2019), and mutations in *PWR* and *HOS15* resulted in delayed vegetative phase change (Cheng *et al.*, 2021), suggesting the presence of a complex including PKL, HDA9, PWR and HOS15. A recent study indicated that cell division plays an important role in regulating the expression of *MIR156C*, and reported that HDA9 contributes to a cell division-dependent

decline in H3K27ac at *MIR156C* (Cheng *et al.*, 2021). It will be important to determine if, and how, cell division affects the association of HDA9 with this gene.

PKL and histone deacetylases act in multiple pathways to regulate vegetative phase change

Although HDA6 regulates vegetative phase change, it does not appear to directly regulate miR156 nor SPL9. It could regulate *SPL* genes independently of miR156 or regulate genes downstream of the miR156-SPL module. The genetic interaction between *pkl-10* and *hda6-7* is synergistic, supporting the idea that PKL and HDA6 function in multiple pathways to regulate vegetative phase change. HDA9 is bound to *MIR156A/MIR156C* in 1-wk-old and 2-wk-old plants and is more abundant at these genes at 2 wk. The association of HDA9 with *MIR156A/MIR156C* declined to basal levels at 3 wk, which was consistent with the observation that H3K27ac reaches its lowest level at these genes at 3 wk (Xu *et al.*, 2016a). PKL, however, binds to *MIR156A/MIR156C* constantly from 1 to 3 wk (Xu *et al.*, 2016a). The different binding affinity between PKL and HDA9 at *MIR156A/MIR156C* and the addictive genetic interaction between *pkl-10* and *hda9-1* suggested that PKL and HDA9 function in overlapping and different pathways to regulate vegetative phase change.

Action of PKL and HDA9 on histone modifications

Western blot analysis showed that HDA9 reduces H3K27ac globally, and the H3K27ac levels at *MIR156A/MIR156C* were significantly increased in 1-wk-old *hda9-1*. Removing acetylation at H3K27 may facilitate the methylation of H3K27. However, we did not observe statistically significant global reduction of H3K27me3 in *hda9-1*. HDA9 associates with PKL, and PKL does not modulate H3K27me3 globally. Nevertheless, PKL does regulate H3K27me3 levels at some loci, such as the seed specific gene *LEAFY COTYLEDON1* (*LEC1*) and *LEC2*, flowering time genes *FRUITFUL* and *AGAMOUS-LIKE24*, and vegetative phase change genes *MIR156A/MIR156C* (Zhang *et al.*, 2008, 2012; Xu *et al.*, 2016a). Similarly, HDA9 regulates H3K27me3 levels at some target genes such as *FLC* (Zeng *et al.*, 2020). Analysis of H3K27ac and H3K27me3 levels at *MIR156A/MIR156C* suggested that reduction in H3K27ac levels did not necessarily result in increased H3K27me3 levels. H3K27me3 levels were significantly reduced in 2-wk-old and 3-wk-old *pkl-10* at *MIR156C* near its TSS and regions that are downstream of the TSS, but were only slightly reduced at the TSS of *MIR156A*. This suggested that PRC2 activities were differently promoted at *MIR156A* and *MIR156C*. PKL and HDA9 promoted the binding of PRC2 across *MIR156C*, while the binding of PRC2 at *MIR156A* requires other factors. Although PKL and HDA9 did not affect H3K27me3 globally, they both promote H2Aub globally (catalysed by the activities of PRC1), suggesting that PKL and HDA9 may generally promote PRC1 activities at their targets to maintain gene repression. Consistent with this, H3K27me3 levels were not significantly reduced in *hda9-1* at *MIR156A*, but the H2Aub levels were significantly reduced in *hda9-1* at *MIR156A*. HDA9 was reported to physically interact with VAL1, and VAL1 is a B3 domain transcription factor that recruits PRC1 (C. Yang *et al.*, 2013; Wu *et al.*, 2018; Zeng *et al.*, 2020). Together with other reports that suggest that PRC2 can act before, after, or independently of PRC1 (C. Yang *et al.*, 2013; Qüesta *et al.*, 2016; Zhou *et al.*, 2017), our results suggested that PKL and HDA9 probably promote PRC1 activities to increase H2Aub levels at both *MIR156A/MIR156C*, which is sufficient to promote PRC2 activities at *MIR156C*, while the promoting of PRC2 activities at *MIR156A* requires other factors.

Overall, HDA9 is temporally recruited to *MIR156A/MIR156C* to mediate the downregulation of *MIR156A/MIR156C*, while HDA6 does not regulate miR156 nor SPL9 directly. PKL associates with HDA6 and HDA9, and possibly also with other histone deacetylases, to promote H2Aub and H3K27me3 at *MIR156A/MIR156C* to mediate and maintain the repression of *MIR156A/MIR156C*. This might be very important for biennial and perennial plants: once the vegetative phase change has occurred in the plant, the plant will be maintained in the adult phase such that the plant would not restart the juvenile development in the next growing season.

Acknowledgements

We thank Scott Poethig and Beth Krizek for critical reading of this manuscript. This work was supported by a grant from the National Science Foundation (IOS 1947274) and startup funds from the University of South Carolina to MX. The authors declare no conflict of interest.

Author contributions

TH and MX planned and designed the research, performed experiments and analysed data. DM and VH performed genotyping experiments. MX wrote the manuscript. All authors read and approved the manuscript.

ORCID

Mingli Xu https://orcid.org/0000-0001-7997-573X

Data availability

The data that support the findings of this study are available in the supplementary material of this article.

References

Aichinger E, Villar CB, Di Mambro R, Sabatini S, Köhler C. 2011. The CHD3 chromatin remodeler PICKLE and polycomb group proteins antagonistically regulate meristem activity in the *Arabidopsis* root. *Plant Cell* **23**: 1047–1060.

Aichinger E, Villar CB, Farrona S, Reyes JC, Hennig L, Köhler C. 2009. CHD3 proteins and polycomb group proteins antagonistically determine cell identity in *Arabidopsis*. *PLoS Genetics* **5**: e1000605.

Angel A, Song J, Dean C, Howard M. 2011. A polycomb-based switch underlying quantitative epigenetic memory. *Nature* **476**: 105–108.

Aufsatz W, Mette MF, van der Winden J, Matzke M, Matzke AJ. 2002. HDA6, a putative histone deacetylase needed to enhance DNA methylation induced by double-stranded RNA. *EMBO Journal* **21**: 6832–6841.

Buendía-Monreal M, Gillmor CS. 2017. Convergent repression of miR156 by sugar and the CDK8 module of *Arabidopsis* Mediator. *Developmental Biology* **423**: 19–23.

Chen X, Lu L, Mayer KS, Scalf M, Qian S, Lomax A, Smith LM, Zhong X. 2016. POWERDRESS interacts with HISTONE DEACETYLASE 9 to promote aging in *Arabidopsis*. *eLife* **22**: e17214.

Cheng YJ, Shang GD, Xu ZG, Yu S, Wu LY, Zhai D, Tian SL, Gao J, Wang L, Wang JW. 2021. Cell division in the shoot apical meristem is a trigger for miR156 decline and vegetative phase transition in *Arabidopsis*. *Proceedings of the National Academy of Sciences, USA* **118**: e2115667118.

Choi K, Zhao X, Kelly KA, Venn O, Higgins JD, Yelina NE, Hardcastle TJ, Ziolkowski PA, Copenhaver GP, Franklin FCH *et al.* 2013. *Arabidopsis* meiotic crossover hot spots overlap with H2A.Z nucleosomes at gene promoters. *Nature Genetics* **45**: 1327–1336.

Coustham V, Li P, Strange A, Lister C, Song J, Dean C. 2012. Quantitative modulation of polycomb silencing underlies natural variation in vernalization. *Science* **337**: 584–587.

Deng W, Buzas DM, Ying H, Robertson M, Taylor J, Peacock WJ, Dennis ES, Helliwell C. 2013. *Arabidopsis* polycomb repressive complex 2 binding sites contain putative GAGA factor binding motifs within coding regions of genes. *BMC Genomics* **14**: 593.

Earley K, Lawrence RJ, Pontes O, Reuther R, Enciso AJ, Silva M, Neves N, Gross M, Viegas W, Pikaard CS. 2006. Erasure of histone acetylation by *Arabidopsis* HDA6 mediates large-scale gene silencing in nucleolar dominance. *Genes & Development* **20**: 1283–1293.

Engler C, Youles M, Gruetzner R, Ehnert TM, Werner S, Jones JD, Patron NJ, Marillonnet S. 2014. A golden gate modular cloning toolbox for plants. *ACS Synthetic Biology* **3**: 839–843.

Fouracre JP, He J, Chen VJ, Sidoli S, Poethig RS. 2021. VAL genes regulate vegetative phase change via miR156-dependent and independent mechanisms. *PLoS Genetics* **17**: e1009626.

Gillmor CS, Silva-Ortega CO, Willmann MR, Buendía-Monreal M, Poethig RS. 2014. The *Arabidopsis* mediator CDK8 module genes CCT (MED12) and GCT (MED13) are global regulators of developmental phase transitions. *Development* **141**: 4580–4589.

Guo C, Jiang Y, Shi M, Wu X, Wu G. 2021. ABI5 acts downstream of miR159 to delay vegetative phase change in *Arabidopsis*. *New Phytologist* **231**: 339–350.

Guo C, Xu Y, Shi M, Lai Y, Wu X, Wang H, Zhu Z, Poethig RS, Wu G. 2017. Repression of miR156 by miR159 regulates the timing of the juvenile-to-adult transition in *Arabidopsis*. *Plant Cell* **29**: 1293–1304.

He J, Xu M, Willmann MR, McCormick K, Hu T, Yang L, Starker CG, Voytas DF, Meyers BC, Poethig RS. 2018. Threshold-dependent repression of SPL gene expression by miR156/miR157 controls vegetative phase change in *Arabidopsis thaliana*. *PLoS Genetics* **14**: e1007337.

Ho KK, Zhang H, Golden BL, Ogas J. 2013. PICKLE is a CHD subfamily II ATP-dependent chromatin remodeling factor. *Biochimica et Biophysica Acta* **1829**: 199–210.

Hyun Y, Vincent C, Tilmes V, Bergonzi S, Kiefer C, Richter R, Martinez-Gallegos R, Severing E, Coupland G. 2019. A regulatory circuit conferring varied flowering response to cold in annual and perennial plants. *Science* **363**: 409–412.

Jiao Y, Wang Y, Xue D, Wang J, Yan M, Liu G, Dong G, Zeng D, Lu Z, Zhu X *et al.* 2010. Regulation of OsSPL14 by OsmiR156 defines ideal plant architecture in rice. *Nature Genetics* **42**: 541–544.

Kim YJ, Wang R, Gao L, Li D, Xu C, Mang H, Jeon J, Chen X, Zhong X, Kwak JM *et al.* 2016. POWERDRESS and HDA9 interact and promote histone H3 deacetylation at specific genomic sites in *Arabidopsis*. *Proceedings of the National Academy of Sciences, USA* **113**: 14858–14863.

Lafos M, Kroll P, Hohenstatt ML, Thorpe FL, Clarenz O, Schubert D. 2011. Dynamic regulation of H3K27 trimethylation during *Arabidopsis* differentiation. *PLoS Genetics* **7**: e1002040.

Lawrence EH, Springer CJ, Helliker BR, Poethig RS. 2020. miR156-mediated changes in leaf composition lead to altered photosynthetic traits during vegetative phase change. *New Phytologist* **231**: 1008–1022.

Leichty AR, Poethig RS. 2019. Development and evolution of age-dependent defenses in ant-acacias. *Proceedings of the National Academy of Sciences, USA* **116**: 15596–15601.

Li C, Chen C, Gao L, Yang S, Nguyen VI, Shi X, Siminovitch K, Kohalmi SE, Huang S, Wu K *et al.* 2015. The *Arabidopsis* SWI2/SNF2 chromatin Remodeler BRAHMA regulates polycomb function during vegetative development and directly activates the flowering repressor gene SVP. *PLoS Genetics* **11**: e1004944.

Li HC, Chuang K, Henderson JT, Rider SD Jr, Bai Y, Zhang H, Fountain M, Gerber J, Ogas J. 2005. PICKLE acts during germination to repress expression of embryonic traits. *The Plant Journal* **44**: 1010–1022.

Mao YB, Liu YQ, Chen DY, Chen FY, Fang X, Hong GJ, Wang LJ, Wang JW, Chen XY. 2017. Jasmonate response decay and defense metabolite accumulation contributes to age-regulated dynamics of plant insect resistance. *Nature Communications* **8**: 13925.

Mayer KS, Chen X, Sanders D, Chen J, Jiang J, Nguyen P, Scalf M, Smith LM, Zhong X. 2019. HDA9-PWR-HOS15 Is a core histone deacetylase complex regulating transcription and development. *Plant Physiology* **180**: 342–355.

Park HJ, Baek D, Cha JY, Liao X, Kang SH, McClung CR, Lee SY, Yun DJ, Kim WY. 2019. HOS15 interacts with the histone deacetylase HDA9 and the evening complex to epigenetically regulate the floral activator GIGANTEA. *Plant Cell* **31**: 37–51.

Picó S, Ortiz-Marchena MI, Merini W, Calonje M. 2015. Deciphering the role of POLYCOMB REPRESSIVE COMPLEX1 variants in regulating the acquisition of flowering competence in *Arabidopsis*. *Plant Physiology* **168**: 1286–1297.

Poethig RS. 2003. Phase change and the regulation of developmental timing in plants. *Science* **301**: 334–336.

Poethig RS. 2013. Vegetative phase change and shoot maturation in plants. *Current Topics in Developmental Biology* **105**: 125–152.

Probst AV, Fagard M, Proux F, Mourrain P, Boutet S, Earley K, Lawrence RJ, Pikaard CS, Murfett J, Furner I *et al.* 2004. *Arabidopsis* histone deacetylase HDA6 is required for maintenance of transcriptional gene silencing and determines nuclear organization of rDNA repeats. *Plant Cell* **16**: 1021–1034.

Qüesta JI, Song J, Geraldo N, An H, Dean C. 2016. *Arabidopsis* transcriptional repressor VAL1 triggers polycomb silencing at FLC during vernalization. *Science* **353**: 485–488.

Tamada Y, Yun JY, Woo SC, Amasino RM. 2009. ARABIDOPSIS TRITHORAX-RELATED7 is required for methylation of lysine 4 of histone H3 and for transcriptional activation of FLOWERING LOCUS C. *Plant Cell* **21**: 3257–3269.

Tanaka M, Kikuchi A, Kamada H. 2008. The *Arabidopsis* histone deacetylases HDA6 and HDA19 contribute to the repression of embryonic properties after germination. *Plant Physiology* **146**: 149–161.

Telfer A, Bollman KM, Poethig RS. 1997. Phase change and the regulation of trichome distribution in *Arabidopsis thaliana*. *Development* **124**: 645–654.

Tian R, Wang F, Zheng Q, Niza V, Downie AB, Perry SE. 2020. Direct and indirect targets of the *arabidopsis* seed transcription factor ABSCISIC ACID INSENSITIVE3. *The Plant Journal* **103**: 1679–1694.

Turck F, Roudier F, Farrona S, Martin-Magniette ML, Guillaume E, Buisine N, Gagnot S, Martienssen RA, Coupland G, Colot V. 2007. *Arabidopsis* TFL2/LHP1 specifically associates with genes marked by trimethylation of histone H3 lysine 27. *PLoS Genetics* **3**: e86.

Wang J, Zhou L, Shi H, Chern M, Yu H, Yi H, He M, Yin J, Zhu X, Li Y *et al.* 2018. A single transcription factor promotes both yield and immunity in rice. *Science* **361**: 1026–1028.

Wang JW, Park MY, Wang LJ, Koo Y, Chen XY, Weigel D, Poethig RS. 2011. miRNA control of vegetative phase change in trees. *PLoS Genetics* **7**: e1002012.

Wang JW, Schwab R, Czech B, Mica E, Weigel D. 2008. Dual effects of miR156-targeted SPL genes and CYP78A5/KLUH on plastochron length and organ size in *Arabidopsis thaliana*. *Plant Cell* **20**: 1231–1243.

Willmann MR, Poethig RS. 2007. Conservation and evolution of miRNA regulatory programs in plant development. *Current Opinion in Plant Biology* **10**: 503–511.

Wood CC, Robertson M, Tanner G, Peacock WJ, Dennis ES, Helliwell CA. 2006. The *Arabidopsis thaliana* vernalization response requires a polycomb-like

protein complex that also includes VERNALIZATION INSENSITIVE 3. *Proceedings of the National Academy of Sciences, USA* **103**: 14631–14636.

van der Woude LC, Perrella G, Snoek BL, van Hoogdalem M, Novák O, van Verk MC, van Kooten HN, Zorn LE, Tonckens R, Dongus JA *et al.* 2019. HISTONE DEACETYLASE 9 stimulates auxin-dependent thermomorphogenesis in *Arabidopsis thaliana* by mediating H2A.Z depletion. *Proceedings of the National Academy of Sciences, USA* **116**: 25343–25354.

Wu B, Zhang M, Su S, Liu H, Gan J, Ma J. 2018. Structural insight into the role of VAL1 B3 domain for targeting to FLC locus in *Arabidopsis thaliana*. *Biochemical and Biophysical Research Communications* **501**: 415–422.

Wu G, Park MY, Conway SR, Wang JW, Weigel D, Poethig RS. 2009. The sequential action of miR156 and miR172 regulates developmental timing in *Arabidopsis*. *Cell* **138**: 750–759.

Xu M, Hu T, Smith MR, Poethig RS. 2016a. Epigenetic regulation of vegetative phase change in *Arabidopsis*. *Plant Cell* **28**: 28–41.

Xu M, Hu T, Zhao J, Park MY, Earley KW, Wu G, Yang L, Poethig RS. 2016b. Developmental functions of miR156-regulated SQUAMOSA PROMOTER BINDING PROTEIN-LIKE (SPL) genes in *Arabidopsis thaliana*. *PLoS Genetics* **12**: e1006263.

Xu M, Hu T, Poethig RS. 2021. Low light intensity delays vegetative phase change. *Plant Physiology* **187**: 1177–1188.

Xu M, Leichty AR, Hu T, Poethig RS. 2018. H2A.Z promotes the transcription of MIR156A and MIR156C in *Arabidopsis* by facilitating the deposition of H3K4me3. *Development* **145**: dev152868.

Xu Y, Guo C, Zhou B, Li C, Wang H, Zheng B, Ding H, Zhu Z, Peragine A, Cui Y *et al.* 2016. Regulation of vegetative phase change by SWI2/SNF2 chromatin remodeling ATPase BRAHMA. *Plant Physiology* **172**: 2416–2428.

Yang C, Bratzel F, Hohmann N, Koch M, Turck F, Calonje M. 2013. VAL- and AtBMI1-mediated H2Aub initiate the switch from embryonic to postgerminative growth in *Arabidopsis*. *Current Biology* **23**: 1324–1329.

Yang L, Chen X, Wang Z, Sun Q, Hong A, Zhang A, Zhong X, Hua J. 2020. HOS15 and HDA9 negatively regulate immunity through histone deacetylation of intracellular immune receptor NLR genes in *Arabidopsis*. *New Phytologist* **226**: 507–522.

Yang L, Xu M, Koo Y, He J, Poethig RS. 2013. Sugar promotes vegetative phase change in *Arabidopsis thaliana* by repressing the expression of MIR156A and MIR156C. *eLife* **2**: e00260.

Yu S, Cao L, Zhou CM, Zhang TQ, Lian H, Sun Y, Wu J, Huang J, Wang G, Wang JW. 2013. Sugar is an endogenous cue for juvenile-to-adult phase transition in plants. *eLife* **2**: e00269.

van Zanten M, Zöll C, Wang Z, Philipp C, Carles A, Li Y, Kornet NG, Liu Y, Soppe WJ. 2014. HISTONE DEACETYLASE 9 represses seedling traits in *Arabidopsis thaliana* dry seeds. *The Plant Journal* **80**: 475–488.

Zeng X, Gao Z, Jiang C, Yang Y, Liu R, He Y. 2020. HISTONE DEACETYLASE 9 functions with polycomb silencing to repress FLOWERING LOCUS C expression. *Plant Physiology* **182**: 555–565.

Zhang H, Bishop B, Ringenberg W, Muir WM, Ogas J. 2012. The CHD3 remodeler PICKLE associates with genes enriched for trimethylation of histone H3 lysine 27. *Plant Physiology* **159**: 418–432.

Zhang H, Rider SD, Henderson JT, Fountain M, Chuang K, Kandachar V, Simons A, Edenberg HJ, Romero-Severson J, Muir WM *et al.* 2008. The CHD3 remodeler PICKLE promotes trimethylation of histone H3 lysine 27. *Journal of Biological Chemistry* **283**: 22637–22648.

Zhang X, Clarenz O, Cokus S, Bernatavichute YV, Pellegrini M, Goodrich J, Jacobsen SE. 2007a. Whole-genome analysis of histone H3 lysine 27 trimethylation in *Arabidopsis*. *PLoS Biology* **5**: e129.

Zhang X, Germann S, Blus BJ, Khorasanizadeh S, Gaudin V, Jacobsen SE. 2007b. The *Arabidopsis* LHP1 protein colocalizes with histone H3 Lys27 trimethylation. *Nature Structural & Molecular Biology* **14**: 869–871.

Zhou Y, Romero-Campero FJ, Gómez-Zambrano Á, Turck F, Calonje M. 2017. H2A monoubiquitination in *Arabidopsis thaliana* is generally independent of LHP1 and PRC2 activity. *Genome Biology* **18**: 69.

Supporting Information

Additional Supporting Information may be found online in the Supporting Information section at the end of the article.

Fig. S1 HDA6 does not bind to *SPL9* directly.

Fig. S2 Complementation assay of transgenic plants.

Fig. S3 Genetic interaction between PICKLE (PKL) and HDA6, and PKL and HDA9.

Fig. S4 Western blot analysis of H3K27ac, H3K27me3 and H2Aub in 2-wk-old shoot apices of Col, *hda9-1*, *pkl-10* and *pkl-10 hda9-1* in two biological replicates.

Table S1 Primers used in this study.

Please note: Wiley Blackwell are not responsible for the content or functionality of any Supporting Information supplied by the authors. Any queries (other than missing material) should be directed to the *New Phytologist* Central Office.